Towards integrated position sensors with nanometer precision

Sebastian Schulz, Paul Beck, Laura Wynne, Simone Iadanza, Liam O'Faolain, et al.

Sebastian A. Schulz, Paul Beck, Laura C. Wynne, Simone Iadanza, Liam O'Faolain, Peter Banzer, "Towards integrated position sensors with nanometer precision," Proc. SPIE 12334, Emerging Applications in Silicon Photonics III, 1233405 (11 January 2023); doi: 10.1117/12.2644959

SPIE.

Event: SPIE Photonex, 2022, Birmingham, United Kingdom

Towards integrated position sensors with nanometer precision

Sebastian A. Schulz[a], Paul Beck[b,c], Laura C. Wynne[a], Simone Iadanza[d,e], Liam O'Faolain[d,e], and Peter Banzer[b,c,f]

[a]SUPA, School of Physics and Astronomy, University of St Andrews, North Haugh, KY16 9SS, St Andrews, UK
[b]Max Planck Institute for the Science of Light, Staudtstr. 2, D-91058 Erlangen, Germany
[c]Institute of Optics, Information and Photonics, Department of Physics, Friedrich-Alexander-University Erlangen-Nuremberg, Staudtstr. 7/B2, D-91058 Erlangen, Germany
[d]Centre for Advanced Photonics & Process Analysis, Munster Technological University, Bishopstown, T12 P928 Cork, Ireland
[e]Tyndall National Institute, Lee Maltings, Dyke Parade, T12 R5CP, Cork, Ireland
[f]Institute of Physics, University of Graz, NAWI Graz, Universitätsplatz 5, Graz, 8010 Austria

ABSTRACT

The ability to precisely measure the displacement between two elements, e.g. a mask and a substrate or a beam and optical elements, is fundamental to many precision experiments and processes. Yet typical optical displacement sensors struggle to go significantly below the diffraction limit. Here we combine advances in our understanding of directional scattering from nanoparticles with silicon photonic waveguides to demonstrate a displacement sensor with deep subwavelength accuracy. Depending on the level of integration and waveguide geometry used we achieve a spatial resolution between $5-7\,\mathrm{nm}$, equivalent to approximately $\lambda/200-\lambda/300$.

Keywords: silicon photonics, directional scattering, sensors, integrated optics, photonic integrated circuits

1. INTRODUCTION

Within the field of optics and photonics, many processes rely on the precise alignment between either two elements or an optical beam to an optical element. Examples include but are not limited to the alignment between optical fibres and integrated waveguides in the packaging of Photonic integrated circuits, aligning the mask and substrate of UV or nanoimprint lithography systems, or measuring the precise displacement of a stage in electron beam lithography or precision microscopy. Yet our technological solutions here are limited and often provide barely sufficient accuracy. E.g. typical lithography alignment involves the use of matching or complementary patterns, such as Moire gratings, split across the substrate and mask, with either machine vision or a skilled operator required to achieve precise alignment. This results in repeatability issues and typical alignment accuracies on the order of 100s nm.[1] Similar alignment accuracies can also be achieved in electron beam lithography, where the mechanical displacement of a stage is measured using an optical interferometer. With optical structures having dimensions of a similar order it is clear that such alignment accuracy is a major limiting factor. Here we thus present a novel approach to optical displacement sensors, measuring the displacement between a reference beam and a silicon photonics chip. Our approach is based on directional (Kerker) scattering from a Huygens dipole - a nanoparticle that simultaneously features an electric and magentic dipole, with a controlled phase and amplitude relation.[2–4] This dipole is then coupled to a set of integrated photonic waveguides and the relative signal between two opposite directions is used to determine the displacement along multiple axes. We present multiple generations of this device, featuring different levels of integration and show that in a monolithically integrated system the achievable accuracy is approximately 7 nm.

Further author information: Send correspondence to S.A.S
E-mail: sas35@st-andrews.ac.uk, Telephone: 01334463196

Emerging Applications in Silicon Photonics III, edited by Callum G. Littlejohns, Marc Sorel,
Proc. of SPIE Vol. 12334, 1233405 · © 2023 SPIE · 0277-786X
doi: 10.1117/12.2644959

2. WORKING PRINCIPLES

2.1 Directional scattering

Here we look at the theoretical concept underlying our displacement sensor. As we will discuss in section 3 we illuminate our sensor with a tightly focused radially polarized beam. In the collimated case such a beam has an electric field component E_r and magnetic field H_ϕ. When focused this results in an additional E_z component, with all other components (E_ϕ, H_r, and H_z) equal to zero. The nanoparticle at the centre of our sensor will act as a Mie scatterer and hence the focused radially polarized beam will excite both an electric and magnetic dipole simultaneously. The direction of the magnetic dipole as well as the phase and amplitude relation between these two dipoles, which depends on the displacement between the scatterer and the centre of the incident beam, control the direction into which this pair of dipoles emits, see Fig.1. For a particle at the centre of the beam, this results in only E_z excitation and hence symmetric scattering within the radial plane (plane of the sample). However, as the scatterer is shifted of centre the E_z-component reduces and the magnetic field component increases. This results in directional scattering dependent on both the direction and magnitude of the displacement.

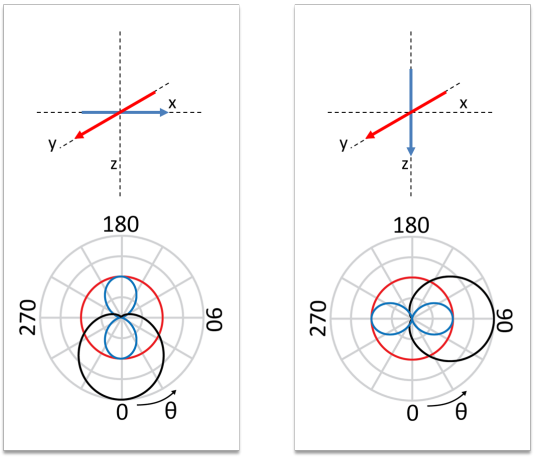

Figure 1. Schematics showing how the direction of emission is dependent on the orientation of two dipoles.

2.2 Semi-integrated Kerker scatter

In this report, we will discuss two device geometries, one which is partially integrated,[5] and one fully integrated.[6] In the partially integrated version, a spherical silicon nanoparticle (with radius $r \sim 260$nm) is placed on the centre of a crossing of three photonic crystal waveguides. The photonic crystal geometry is chosen such that we have a significant overlap (in k-space) between the light scattered by the nanoparticle and the photonic crystal waveguide mode. It is a triangular lattice of air holes in silicon, with a period $a = 424\,\text{nm}$ and hole radius $R_{hole} = 0.275a$. The waveguide is formed by removing a single row of holes, i.e. a W1 waveguide.[7] The waveguides are terminated in a tapered end, followed by a scattering edge, such that the light scattered from this edge can be imaged using a vertical microscope.

2.3 Integrated version

The second implementation discussed here is a monolithically integrated version. In this case, the scatterer consists of a silicon cylinder, at the centre of a cross formed by two photonic wire waveguides (fully etched, 490 nm width). To increase the coupling efficiency the waveguides are tapered at the centre to a width of 550 nm as well as at being terminated in an inverse taper, to form the same outcoupling geometry as used for the semi-integrated version. Scanning electron microscope images of both devices are shown in Fig.2.

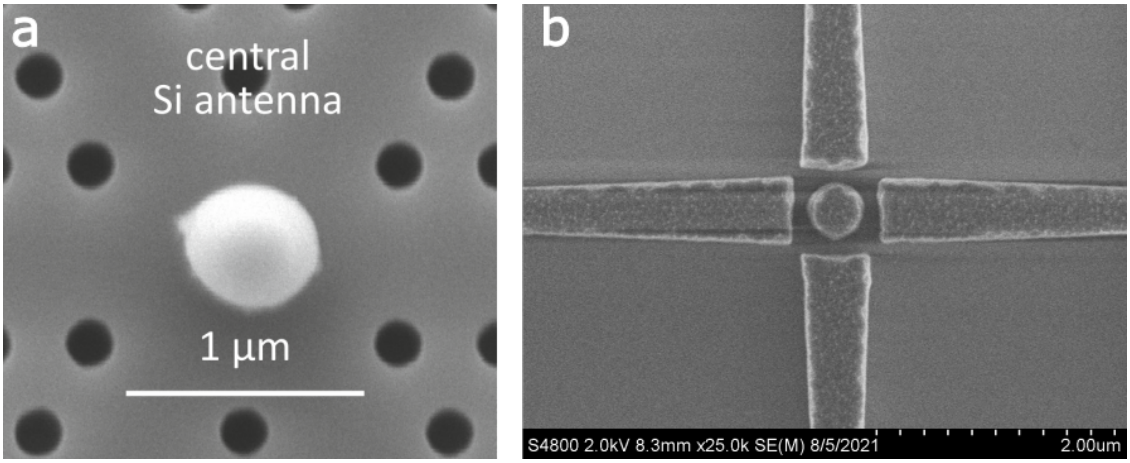

Figure 2. Scanning electron microscope images of the two implementations. a) A silicon nanosphere is placed on the centre of a PhC waveguide crossing. b) An etched silicon cylinder at the centre of a photonic wire crossing.

3. FABRICATION AND CHARACTERISATION

3.1 Fabrication

Both versions of the displacement sensor follow the same overall fabrication protocol. The devices are fabricated in 220 nm Silicon on 2 μm of buried oxide (SOITEC smartcut wafers). The patterns are defined in a layer of ZEP520A electron beam resist using a 30 kV, Raith electron beam lithography system. After the development of the resist, the pattern is then transferred into the silicon layer via reactive ion etching using equal parts of CHF_3 and SF_6 gas. The remaining resist is then removed using 1165 resist stripper. Following this step, the fabrication approach for both devices differs. For the semi-integrated displacement sensor, the buried oxide is removed using a concentrate Hydrofluoric acid wet etch, and then the silicon nanoparticle is placed at the centre of the waveguide crossing via pick-and-place in a scanning electron microscope equipped with nanomanipulators. The fully integrated version of the device on the other hand requires a symmetric index distrubtion around the nanoparticle, hence a 2 μm cladding is deposited via repeat spin coating and hardbaking of Accuglass.

3.2 Experimental setup

For the experimental characterisation, the sample is placed at the sample plane of an optical microscope operated in reflection. The radially or azimuthally polarized beam is focused on the nanoparticle using a high numerical aperture microscope objective. The same objective used for focusing the incident beam is also used to collect the light scattered from the waveguide terminations, which is then imaged onto a commercial camera. A circular beam stop is introduced into the imaging arm of the setup, to block reflections from the sensor's centre.

We thus measure the relative intensity of light coming out of the different waveguide terminations, determining a directivity for each waveguide, given by

$$D_i = \frac{P_i^+ - P_i^{-\prime}}{P_i^+ + P_i^-}$$

where the index i corresponds to either 0, 60 or 120 degrees for the photonic crystal waveguide crossing and the x and y-axis for the wire crossing respectively, and P_i^+ and P_i^- are the outcoupled powers at opposites end of the i- waveguide. This directivity value is normalised, thus accounting for possible variations in total coupled power, and takes a range from -1 to 1 for each waveguide. We raster scan the sample, through the microscope, measuring the directivity for all waveguides at each position. To determine the accuracy of our sensor we measure the statistical variation of our signal for a given sample position, with standard deviation δD_i. By combining this measurement error on the directivity with the slope of directivity (ΔD_i) vs sample displacement we obtain a measure of the resolution of our displacement sensor,

$$\Delta i = \frac{\delta D_i}{\Delta D_i},$$

where Δi is the smallest resolvable step along the direction of the waveguide denoted by index i.

4. RESULTS

When performing these measurements we observe that the semi-integrated device has a larger slope ΔD_i and standard deviation δD_i than the fully integrated version, with the parameters provided in table 1. We attribute this to two factors. The spherical nanoparticle is a better scatterer for the purpose of the intended transverse Kerker scattering compared to the cylindrical scatterer. Thus the same variation in position gives a larger change in the directionality of the scattered light and hence the observed directivity. However, the standard deviation of this measurement is limited by actual (nm-scale) fluctuations in the sample position relative to the incident beam. Thus the same magnitude of fluctuations also results in a larger standard deviation of the measured directivity. Since the resolution is dependent on the ratio of the two it is therefore almost identical, 7.2 nm for the fully integrated sensor, vs 5 nm for the semi-integrated device.

Table 1. Comparison of the two sensor implementations, showing the standard deviation and resolution for each system

Implementation	ΔD	δD	resolution
semi-integrated	$3.33 \cdot 10^{-3}\,\mathrm{nm}^{-1}$	0.017	5 nm
fully integrated	$2.9 \cdot 10^{-5}\,\mathrm{nm}^{-1}$	$2.2 \cdot 10^{-4}$	7.2 nm

5. CONCLUSION

Using a nanoparticle coupled to a photonic crystal waveguide crossing we have demonstrated displacement sensing with deep-subwavelength accuracy, reaching as low as $\lambda/300$. By replacing the nanoparticel with an etched cylindrical scatterer and the photonic crystal waveguides with convention wire waveguides we have created a monolithically integrated sensor that still features an accuracy of 7.2 nm $\sim \lambda/200$. Thue the simplified fabrication process, and enhanced mechanical stability comes at only a minor performance penalty.

This device presents an important step on the path to compact, silicon photonics based displacement/alignment sensors for applications such as high-resolution lithography, with potential for two orders of magnitude improvement compared to current aligment technology.

REFERENCES

[1] EVGroup, "EVG IQ Aligner NT: Automated Mask Alignment System." https://www.evgroup.com/fileadmin/media/products/lithography/mask_alignment/iqalignernt/EVG_IQ_Aligner_NT_Flyer.pdf. accessed: 15.09.2022.

[2] Kerker, M., Wang, D.-S., and Giles, C., "Electromagnetic scattering by magnetic spheres," *JOSA* **73**(6), 765–767 (1983).

[3] Neugebauer, M., Woźniak, P., Bag, A., Leuchs, G., and Banzer, P., "Polarization-controlled directional scattering for nanoscopic position sensing," *Nature communications* **7**, 11286 (2016).

[4] Bag, A., Neugebauer, M., Woźniak, P., Leuchs, G., and Banzer, P., "Transverse kerker scattering for angstrom localization of nanoparticles," *Physical review letters* **121**(19), 193902 (2018).

[5] Bag, A., Neugebauer, M., Mick, U., Christiansen, S., Schulz, S. A., and Banzer, P., "Towards fully integrated photonic displacement sensors," *Nature communications* **11**(1), 1–7 (2020).

[6] Beck, P., Wynne, L. C., Iadanza, S., O'Faolain, L., Schulz, S. A., and Banzer, P., "A high-precision silicon-on-insulator position sensor," *under review* .

[7] M.Notomi, A.Shinya, S.Mitsugi, E.Kuramochi, and H-Y.Ryu, "Waveguides, resonators and their coupled elements in photonic crystal slabs," *Optics Express* **12**, 1551 (2004).